

# Molecular Recognition Imaging and Force Spectroscopy of Single Biomolecules

FERRY KIENBERGER,<sup>§</sup> ANDREAS EBNER,<sup>§</sup>  
HERMANN J. GRUBER, AND  
PETER HINTERDORFER\*

*Institute for Biophysics, Johannes Kepler University of Linz,  
Altenbergerstrasse 69, A-4040 Linz, Austria*

Received July 27, 2005

## ABSTRACT

In recent years, considerable attention has focused on biological applications of the atomic force microscope (AFM), in particular on high-resolution imaging of individual biological molecules and on the measurement of molecular forces under near-physiological conditions. The detection of intermolecular forces in the piconewton range has paved the way to investigate details on structural parameters of the binding pockets and the energy landscapes of many biomolecular interactions. The capability of AFM to resolve nanometer-sized details, together with its force detection sensitivity, led to the development of molecular recognition imaging. By a combination of topographical imaging with force measurements, receptor sites are localized with nanometer accuracy. Topography and recognition of target molecules are thereby simultaneously mapped. Thus the AFM can identify specific components in a complex biological sample and retain its high resolution in imaging.

## Introduction

Since its invention in the late 1980s, the atomic force microscope<sup>1</sup> (AFM) has increasingly been used for the visualization of biomolecules and complex biological structures.<sup>2</sup> The main advantage compared to other high-resolution methods such as electron microscopy and X-ray diffraction is that the measurements can be carried out in a fluid environment, including physiological medium, which is crucial to study the structure and function of biomolecules. In particular, the specimen can be imaged in its native state, that is, there is no need to stain, freeze, or crystallize biological samples. The exceptional signal-

to-noise ratio of the AFM allows individual biomolecules to be imaged at sub-nanometer resolution,<sup>3</sup> making it possible to observe single biomolecules at work<sup>4</sup> and to study the function of biomolecular assemblies.<sup>5</sup> In addition to high-resolution imaging of proteins, nucleotides, membranes, and living cells,<sup>6</sup> the measurement of mechanical forces at the molecular level has provided detailed insights into the function and structure of many biomolecular systems.<sup>7–9</sup> Inter- and intramolecular interactions can be studied directly at the molecular level, as exemplified by analysis of the binding potentials of receptor–ligand pairs involved in cell adhesion,<sup>10</sup> polysaccharide elasticity,<sup>11</sup> DNA mechanics,<sup>12</sup> and the function of molecular motors.<sup>13</sup> In case of receptor–ligand complexes, defined forces are exerted on a receptor–ligand complex and the dissociation process is followed over time. Dynamic aspects of recognition are addressed in force spectroscopy experiments, where distinct force–time profiles are applied to monitor changes of conformations and states during receptor–ligand dissociation. Dynamic force spectroscopy, therefore, allows one to detect energy barriers that are difficult or impossible to detect by conventional, near-equilibrium assays and to probe the free energy surface of proteins and molecular complexes.<sup>14</sup>

In the past decade, the resolution of topographical imaging and the force sensitivity have been much improved, mainly due to continuous developments of AFM instrumentation. By combination of topographical imaging with force measurements, receptor sites on a surface are localized with nanometer positional accuracy; thus, topographical images and recognition images are recorded at the same time.<sup>15</sup> AFM also allows one to select particular molecules from a large population. Time-dependent biomolecular processes can be followed on the single molecule level, which allows one to study transient intermediate states and individual reaction pathways without synchronizing large populations of molecules.<sup>16</sup>

This Account details the use of molecular recognition studies for exploring fine kinetic and structural details of molecular recognition processes. Furthermore, the combination of topographical imaging with single molecule force measurements is presented as a new tool for the localization of binding sites on various surfaces. With this methodology, topography and recognition images can be obtained at the same time and distinct receptor sites in the recognition image can be assigned to structures from the topography image. It is applicable to almost any kind of ligand; thus many types of proteins or other biomolecules can be specifically recognized and mapped on cells, membranes, or other subcellular structures.

## Single Molecule Recognition

In molecular recognition experiments, the binding of ligands immobilized on AFM tips toward surface bound

Ferry Kienberger received his Ph.D. in biophysics from the University of Linz in 2002. His postdoctoral work (2002–2003) at the Center for Applied Molecular Engineering and Proceryon Biosciences GmbH, University of Salzburg, focused on structural bioinformatics. He is currently a postdoctoral fellow at University of Linz, working in the field of atomic force microscopy.

Andreas Ebner is an undergraduate student in chemistry working on topography and recognition imaging using the atomic force microscope.

Hermann Gruber obtained his Ph.D. in chemistry from the University of Graz in 1983. After 3 years of postdoctoral research at Purdue University, Indiana (1983–1985), he moved to the Institute of Biophysics at University of Linz to build up the chemistry group. Since 2001, he has been associate professor for bio-analytics working in the field of single-molecule microscopy.

Peter Hinterdorfer received his Ph.D. in biophysics from the University of Linz in 1992. His postdoctoral work at University of Virginia (1992–1993) focused on fluorescence microscopy studies of membrane proteins. He then built up the atomic force microscopy group at the Institute of Biophysics, University of Linz, acting as associate Professor since 1999. His research involves the investigation of single molecular interactions using atomic force microscopy.

\* Corresponding author. Tel: 0043 732 2468 9265. Fax: 0043 732 2468 9270. E-mail: peter.hinterdorfer@jku.at.

<sup>§</sup> Contributed equally to this work.

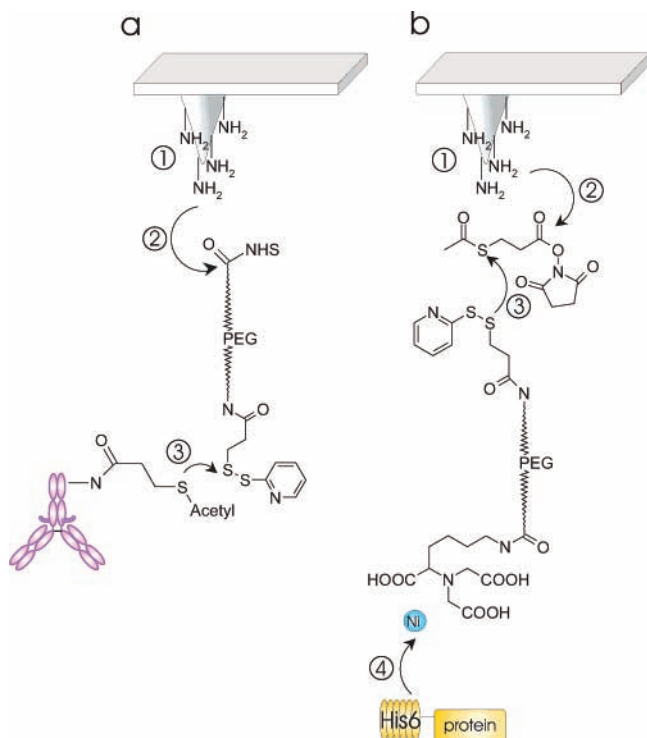


**FIGURE 1.** Linkage of ligands to AFM tips. Ligands were linked to AFM tips via heterobifunctional poly(ethylene glycol) (PEG) derivatives of  $\sim 8$  nm length. Silicon nitride tips were functionalized with ethanolamine (step 1). (a) Covalent linkage via disulfide bond: The amino group on the tip was reacted with the NHS ester function on the PEG linker (step 2). This tip was immersed in a solution of antibody that had been prederivatized with an *S*-acetylthiopropionyl (SATP) group. Removal of the acetyl group with hydroxylamine gave a free thiol, which formed a disulfide bond with the PEG linker (step 3). (b) Noncovalent linkage of His<sub>6</sub>-tagged proteins: The amino groups on the tip were derivatized with SATP groups (step 2), the *S*-acetyl group was removed with hydroxylamine, and the resulting thiol reacted with the pyridyldithio group on the PEG linker (step 3). The His<sub>6</sub>-tagged protein was then bound in the presence of nickel salt (step 4).

receptors (or vice versa) is studied by applying a force to the receptor–ligand complex until the bond breaks at a measurable unbinding force. Such experiments require that one or few ligand molecules are permanently tethered to the apex of the AFM tip, usually by covalent bonding via a flexible linker molecule.<sup>17</sup> The ligand on the linker molecule can freely orient and diffuse within a certain volume provided by the length of the tether, thereby achieving unconstrained binding to its receptor. In the first step of the anchoring protocol, amino groups are generated at a low surface density on the tip, corresponding to few sites per tip apex,<sup>18</sup> as needed for single molecule experiments (Figure 1). In the second step, one end of a distensible and flexible linker (poly(ethylene glycol), PEG) is attached to the amino group on the tip (Figure 1a). In the third step, the ligand (e.g., an antibody) is linked to the outer end of PEG. Cross-linkers with 6–8 nm length (corresponding to 18 ethylene glycol units plus termini) gave a good compromise between high mobility of the ligand and narrow lateral resolution of the target site. The typical PEG linker has one amino-reactive end

for attachment to the tip and one thiol-reactive end for linking of ligands with reactive sulfhydryls (exemplified in Figure 1a).<sup>19</sup> Since the latter are absent in native antibodies, prederivatization of the antibody's lysine residues with the short linker *N*-succinimidyl-3-(*S*-acetylthio)propionate (SATP) is required. Subsequent deprotection with NH<sub>2</sub>OH led to reactive SH groups (Figure 1a). A disadvantage with this method is that it does not allow for site-specific coupling of the cross-linker, since lysine residues are quite abundant. An attractive alternative to covalent coupling is provided by the widely used nitrilotriacetate (NTA)-Ni<sup>2+</sup>-His<sub>6</sub> system (Figure 1b). Fortunately, the binding force of this system is significantly larger than that between most ligand–receptor pairs.<sup>20</sup> Since a His<sub>6</sub> tag is readily appended to proteins, a cross-linker containing a NTA residue is well suited for coupling proteins to the AFM tip (Figure 1b). This generic, site-specific coupling strategy also allows for rigorous and ready control of binding specificity by using Ni<sup>2+</sup> as a molecular switch of the NTA–His<sub>6</sub> bond.

Interaction forces of single ligand–receptor pairs are measured in force–distance cycles using a ligand-carrying tip and a target surface with firmly attached receptor molecules. As a typical example, a force–distance cycle of tip-bound biotin and mica-bound avidin is shown in Figure 2. At a fixed lateral position, the tip vertically approaches the surface and is subsequently retracted. During this cycle, the cantilever deflection,  $x$ , which can be directly converted into a force,  $f$ , according to Hook's law ( $f = kx$ ,  $k$  being the cantilever spring constant), is continuously measured and plotted versus tip–surface separation. At the beginning of the tip–surface approach (Figure 2a, black curve), the cantilever deflection remains zero. Upon tip–surface contact (i.e., at a distance of 0 nm) and further approach, the cantilever bends upward, consistent with a repulsive force that linearly increases with the negative distance. Subsequent tip–surface retraction (Figure 2a, red curve) first leads to relaxation of cantilever bending until the repulsive force drops to zero. Upon further retraction (i.e., at a distance of  $>0$  nm), the cantilever progressively bends downward, reflecting an attractive force between tip-bound biotin and immobilized avidin that increases with increasing tip–surface separation. The shape of this nonlinear force–distance profile is determined by the elastic properties of the flexible PEG cross-linker, whereas the strength of the interaction (termed the unbinding force,  $f_u$ ) is governed by the type of receptor–ligand pair. If the ligand on the tip does not form a bond with the receptor on the surface, the recognition event (i.e., the parabolic shaped curve) is missing and the retrace looks like the trace (Figure 2b). The specificity of ligand–receptor binding is usually demonstrated by blocking experiments with free ligands, which are injected into the solution to block the receptor sites on the surface.<sup>21</sup> As a consequence, all specific recognition signals completely disappear, and only occasionally nonspecific adhesion events are observed.

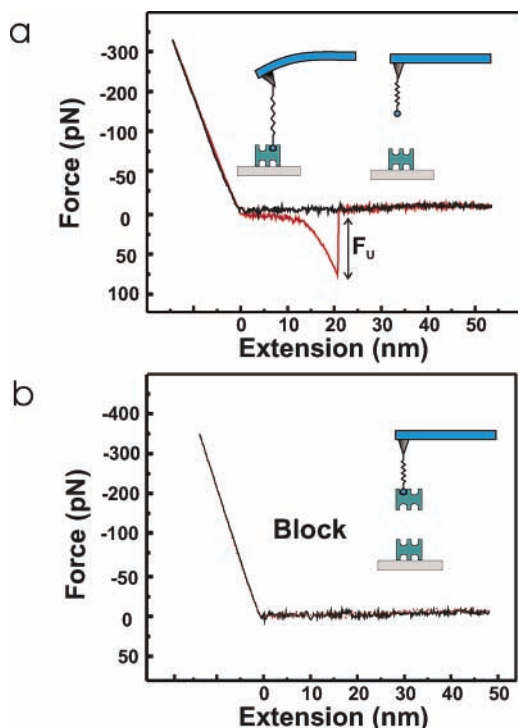


**FIGURE 2.** Principles of single-molecule force measurements. Avidin was adsorbed onto mica, and biotin was attached to an AFM tip via a PEG linker. A force–distance cycle was acquired under buffer conditions. The approach curve (black line) and the retracting curve (red line) are shown. (a) The force–distance cycle exhibits an avidin–biotin unbinding event in the retracting curve with an unbinding force of  $\sim 80$  pN (arrow). The parabolic retraction force curve reflects the extension of the distensible cross-linker–avidin–biotin connection. (b) The specificity of the avidin–biotin unbinding events is shown in blocking experiments where avidin is injected into the solution to block the biotin sites on the AFM tip. As a consequence, the specific recognition signals disappear, and the trace looks like the retrace.

## Molecular Recognition Force Spectroscopy

When ligand–receptor binding is viewed on the single-molecule level, the average lifetime of a ligand–receptor bond at zero force,  $\tau(0)$ , is given by the inverse of the kinetic off-rate constant,  $\tau(0) = 1/k_{\text{off}}$ . Therefore, ligands will dissociate from receptors even without any force applied to the bond at times larger than the average lifetime. In contrast, if molecules are pulled apart very fast, the bond will resist and require a measurable force for detachment.<sup>22</sup> Accordingly, unbinding forces do not constitute unitary values but depend on the dynamics of the unbinding experiments. On the millisecond to second time scale of AFM experiments, thermal impulses govern the unbinding process. In the thermal activation model, the lifetime of a complex in solution is described by a Boltzmann ansatz,  $\tau(0) = \tau_{\text{osc}} \exp(E_{\text{barr}}/(k_{\text{B}}T))$ ,<sup>23</sup> where  $\tau_{\text{osc}}$  is the inverse of the natural oscillation frequency and  $E_{\text{barr}}$  is the energy barrier for dissociation, yielding a simple Arrhenius dependency of dissociation rate on barrier height. A force acting on a binding complex deforms the interaction energy landscape and lowers the activation energy barrier. The lifetime  $\tau(f)$  of a bond loaded with a

constant force  $f$  is given by  $\tau(f) = \tau_{\text{osc}} \exp(E_{\text{barr}} - fx/(k_{\text{B}}T))$ ,<sup>24</sup> with  $x$  being the distance of the energy barrier from the energy minimum along the direction of the applied force. The lifetime under constant force, therefore, compares to the lifetime at zero force, according to  $\tau(f) = \tau(0) \exp(-fx/(k_{\text{B}}T))$ .

With the use of AFM, ligand–receptor unbinding is commonly measured in force–distance cycles, where an effective force increase or loading rate,  $r$ , can be deduced from  $r = df/dt$ , being equal to the product of pulling velocity and effective spring constant. The combination of the Boltzmann ansatz with the stochastic description of the unbinding process predicts the unbinding force distributions at different loading rates  $r$  (Figure 3a).<sup>25</sup> The maximum of each force distribution,  $f^*(r)$ , thereby reflects the most probable unbinding force at the respective loading rate  $r$ .  $f^*$  is related to  $r$  through  $f^*(r) = k_{\text{B}}T/x \ln((rx)/(k_{\text{B}}T k_{\text{off}}))$ . Apparently, the unbinding force  $f^*$  scales linearly with the logarithm of the loading rate. For a single barrier, this would give rise to a simple linear dependence of the force on the logarithm of the loading rate (Figure 3b). In cases where more barriers are involved along the escape path, the curve will follow a sequence of linear regimes, each of which marks a particular barrier.<sup>26</sup> In force spectroscopy experiments, the variation in the pulling speed applied to specific ligand–receptor bonds will lead to detailed structural and kinetic information of the interaction. Length scales of energy barriers are obtained from the slope of the spectroscopy plot (i.e., force versus loading rate) and extrapolation to zero forces yields the kinetic off-rate for the dissociation of the complex in solution.

Various biomolecular interactions have been studied by measuring the loading rate dependence of the unbinding force by changing the pulling velocity of the force exerted to the interaction. The avidin–biotin complex is thereby often regarded as the prototype of a receptor–ligand pair, due to its enormously high affinity ( $K_{\text{D}} = 10^{-13}$  M) and long bond lifetime ( $\tau(0) = 80$  days). First realizations of single-molecule recognition force detections were therefore done with biotin and its cognate receptor avidin, yielding an unbinding force of 160 pN.<sup>7</sup> Recent force-spectroscopy experiments of the avidin–biotin interaction revealed an energy landscape with more than one prominent energy barrier.<sup>26</sup> Using bio-force probe measurements, the loading rate was varied over 8 orders of magnitude, yielding a detailed picture of the force-spectroscopy curve with unbinding forces from 5 pN (at smallest loading rates) to 200 pN (at highest loading rates). Distinct linear regimes that demonstrate the thermally activated nature of the bond breakage are visible, and abrupt changes in slope imply a number of sharp energetic barriers along the dissociation pathway.

In a different study, single-molecule dynamic force spectroscopy was applied to get insights into the binding of Ran, a molecule that regulates assembly and disassembly of the receptor–cargo complexes in the nuclear pore to the nuclear import-receptor importin  $\beta 1$ .<sup>27</sup> By use of recognition force spectroscopy, it was found that the



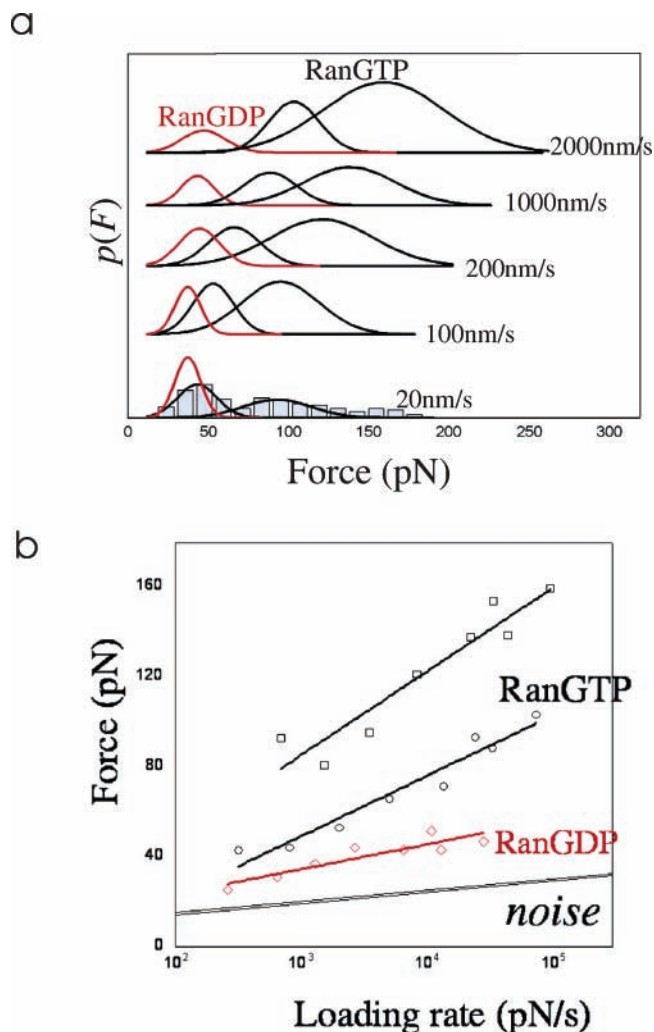


**FIGURE 3.** Dynamic force spectroscopy. Ran and importin  $\beta$  ( $\text{imp}\beta$ ) were immobilized onto the AFM cantilevered tip and mica, respectively, and the interaction force was measured at different loading rates. (a) Unbinding force distributions obtained for  $\text{imp}\beta$ –Ran-GDP (red line) and  $\text{imp}\beta$ –Ran-GTP (black line) complexes at different pulling velocities (ranging from 20 to 2000 nm/s). Association of  $\text{imp}\beta$  with Ran loaded with GDP or with GTP gives rise to uni- or bimodal force distributions, respectively, reflecting the presence of one and two bound states. (b) Force spectra obtained for complexes of  $\text{imp}\beta$  with RanGDP (red line) and RanGTP (black lines), respectively, together with the thermal noise level of the experiments (thick line) (see text for details).

complex of Ran-GTP and importin  $\beta$  alternates between two distinct conformational states with different interaction strength. The force distributions shifted to higher forces by increasing the loading rate, a behavior that fits to the above-mentioned models (Figure 3a). For Ran-GTP, these distributions also had a unique bimodal appearance (two Gaussian fits shown in black at each loading rate in Figure 3a), which cannot be described by the escape from a single potential well. In contrast, a model involving the independent dissociation of two distinct molecular complexes, each leading to a force distribution of its own, accurately fitted the data. The two force populations were shifted to higher forces at increasing loading rates (black

curves in Figure 3b) and also changed in their relative size, with the second (higher-force) population representing a greater fraction at higher loading rates. The results thus indicate that the interaction between Ran-GTP and importin  $\beta$  can lead to two distinctly different bound states, each associated with an individual dissociation pathway.

### Combined Imaging and Force Measurements

Besides measuring interaction strengths, localizing binding sites on biological surfaces such as cells or membranes is also of great interest. To achieve this goal, force detection is combined with topographical imaging. High-resolution imaging together with single-molecule force spectroscopy, therefore, opens new possibilities for analyzing the assembly and function of biomolecular structures.<sup>28</sup> Using a ligand-carrying tip and receptor molecules immobilized onto a flat surface, a complete map of recognition sites can be generated by recording force–distance cycles in every pixel of a defined scan area. This mode, called force-volume, has extensively been used to study adhesion forces of polymer and cell surfaces,<sup>29</sup> ligand–receptor interactions,<sup>30</sup> and specific molecular interactions on living cells.<sup>31</sup> Figure 4a shows a typical recognition force map using an antibody-conjugated tip on a mica substrate with separated lysozyme molecules. The unbinding forces of the individual pixels are shown in gray scale values. Many binding sites on the lysozyme layer were detected, with an average binding probability of 20% in the whole scan area (i.e., 20 out of 100 force–distance cycles showed an unbinding event). The specificity of the binding was shown by adding free antibody in solution, resulting in an effective block of the antibody/antigen interaction (Figure 4b). The binding probability was thereby significantly lowered, as expected for a specific interaction. The measured forces were analyzed and empirical probability density functions (pdf's) were constructed from the unbinding force values (Figure 4c, solid line). The maximum of the distribution ( $\sim 60$  pN) reflects the most probable unbinding force. Upon blocking, binding probabilities were dramatically reduced, as evidenced by the comparison of the pdf before (Figure 4c, solid line) and after blocking (Figure 4c, dotted line).

### Topography and Recognition Imaging, Principles

Although the recognition force map in Figure 4 does indicate the lateral positions of lysozyme molecules on the surface, single molecule resolution is obviously not achieved. The low lateral resolution of force-volume can be overcome by oscillating a modified tip close to its resonance frequency while scanning along the surface. This mode is termed recognition imaging.<sup>32</sup> In this first realization, a tip modified with anti-lysozyme antibodies was used in the dynamic force microscopy mode to scan along a surface loosely covered with lysozyme (Figure 5). Imaging with the antibody-functionalized tip gave strikingly different images than with a bare silicon-nitride tip. Antigenic molecules imaged with the antibody-modified

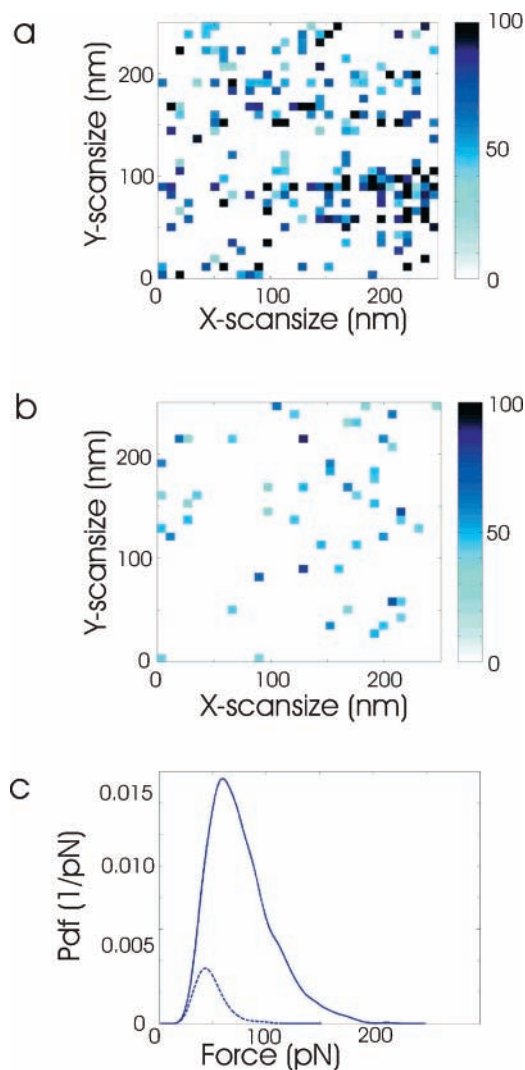


**FIGURE 4.** Combined imaging and force measurements using the force-volume mode. (a) Force-volume data using lysozyme adsorbed onto a mica surface and an anti-lysozyme antibody attached to the tip. Binding sites on the lysozyme layer were detected, and the unbinding forces are scaled in each pixel with gray values (0–100 pN). (b) After blocking with free antibody in solution, the binding probability dropped significantly. (c) Probability density function of the unbinding forces observed in absence (solid line) and in the presence (dotted line) of free antibody in solution. Areas are scaled to binding probabilities.

tip differed significantly both in height and in diameter. The profiles of single lysozyme molecules appeared  $\sim 1$  nm higher and  $\sim 10$  nm broader than profiles from the purely topographical image (i.e., acquired with a bare silicon-nitride tip). Increased heights reflect the amplitude reduction owing to antibody–antigen recognition, whereas increased diameters are due to the additional length of the antibody plus cross-linker molecule. In a row of consecutive images with an antibody-carrying tip and free antigen in solution (Figure 5), the instantaneous switching from recognition images to purely topographical images can be observed. Bright enlarged dots in the first image (Figure 5a) indicate that the antibody on the tip recognizes the antigens on the surface. After some time (Figure 5b, blue arrow), the dots became abruptly smaller both in size

and height, that is, the recognition image turned into a simple topography image. The switching was caused by binding of free lysozyme to the anti-lysozyme on the tip (sketch in Figure 5), thereby blocking the tip-bound antibody and its recognition capability. Subsequent images showed the raw topography of single lysozyme molecules (Figure 5c).

A detailed analysis of the time course of the cantilever oscillations while scanning along the surface is shown in Figure 6. In this experiment, a tip modified with anti-lysozyme antibodies was scanned over mica with adsorbed lysozyme molecules (Figure 6a).<sup>15</sup> As expected, the cantilever oscillated in a nearly sinusoidal fashion according to the preset frequency ( $\sim 7$  kHz) and amplitude ( $\sim 5$  nm peak to peak), Figure 6b. However, both the maxima and minima of the oscillation periods were not strictly constant but were influenced by interactions between tip and sample. On a compressed time scale, only the envelope of the oscillations with its characteristic maxima and minima remained visible (Figure 6c,d). Figure 6c was obtained with a bare tip lacking the anti-lysozyme antibody. The minima varied significantly, showing singly distributed bulges with 10–15 nm width and  $\sim 1$  nm height along the scan axis. These bulges reflect single lysozyme molecules that resisted the further downward movement of the tip toward the surface. In contrast, the positions of the oscillation maxima remained constant, except for minor random variations caused by the thermal noise of the cantilever. Obviously, the information of the surface topography measured with a bare tip is solely contained in the minima of the cantilever oscillations, and cross talk between minima and maxima does not exist at the conditions used (cantilever spring constant 0.1 N/m; Q-factor  $\sim 1$ ; resonance frequency  $\sim 7$  kHz). With a functionalized tip, however (Figure 6d), the maxima were also affected, reflecting restricted tip motion when the PEG linker was bound to the substrate by receptor–ligand recognition. It is important to note that the functionalized tip is still able to yield topographic information, as can be seen from the contour line of the minima in Figure 6d. In conclusion, topographic features and recognitions sites can simultaneously be recorded in a single scan process without mutual interference.

## Topography and Recognition Imaging, Applications

With use of a special electronic circuit (Figure 7a), the minima and the maxima of each sinusoidal cantilever deflection period were separately used for the topography and the recognition image, respectively.<sup>15</sup> With this methodology, topography and recognition images are independently but simultaneously acquired. The topographic image of avidin molecules immobilized onto mica and the simultaneously acquired recognition image using a biotin-modified tip are shown in Figure 7b.<sup>33</sup> Almost all avidin molecules visible in the topographical image (Figure 7b, left panel) were also recognized as dark spots by the biotin–PEG functionalized tip (Figure 7b, right panel),



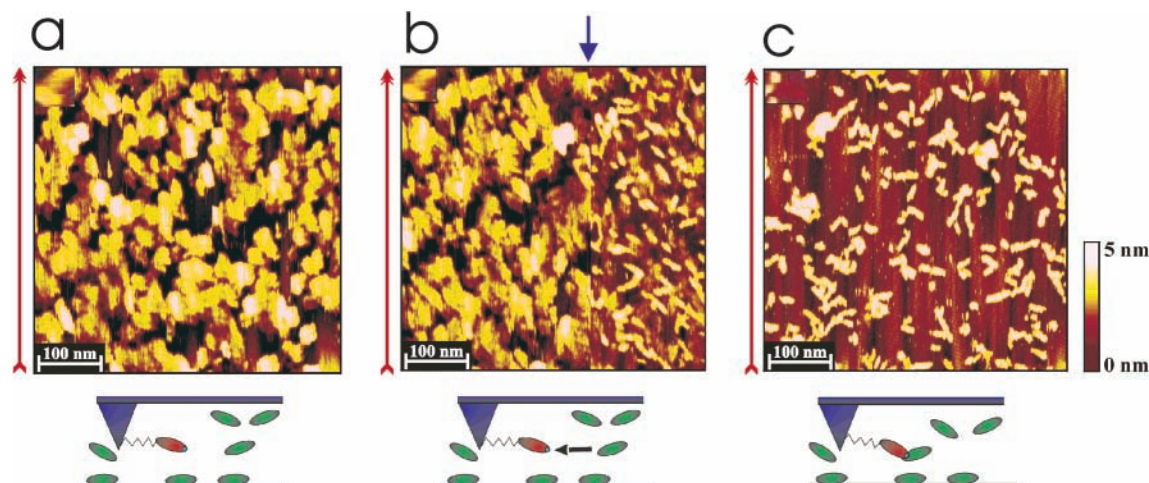


**FIGURE 5.** Antibody recognition imaging. (a) Recognition imaging of single lysozymes using anti-lysozyme antibodies bound to the tip. Antibodies are bound to the tip by a flexible linker (jagged line) for the recognition of lysozyme (shown in green). Due to antibody–antigen interaction, the lysozyme molecules appear higher and broader than in the purely topographical image. (b) Switching of recognition imaging (left part) to pure topography imaging (right part) at a certain time (arrow) in the presence of free antigen in solution. (c) Subsequent images with the blocked tip show the topography of singly distributed lysozyme molecules.

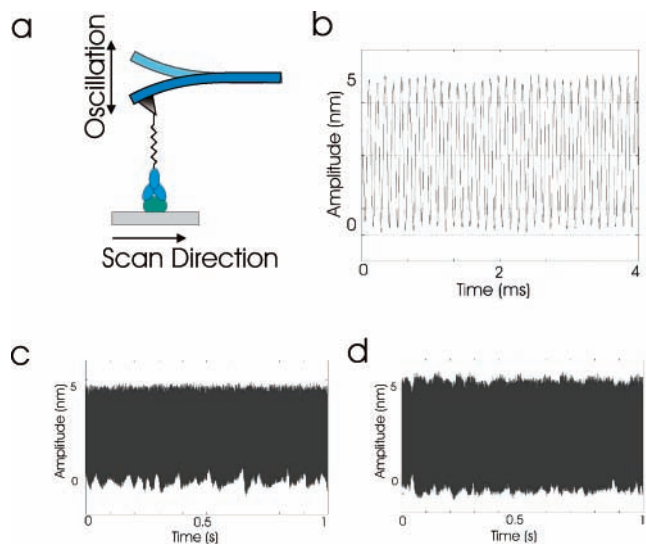


**FIGURE 6.** Principles of recognition imaging. (a) By combination of dynamic force microscopy with single-molecule recognition force spectroscopy, the topography can be investigated together with specific molecular recognition. (b) Deflection signal of a magnetically oscillated cantilever during scanning along the surface (time range 4 ms). The peak to peak amplitude was 5 nm. (c) Deflection signal of a bare tip over a full scan line (time range 1 s). Due to the resulting compression of the time axis, only the extrema of the oscillation periods remain visible. (d) Deflection signal of an anti-lysozyme antibody coated tip scanned over lysozyme molecules (see text for details).

yielding an overall success rate of  $\sim 90\%$ . The good correlation between topography and recognition images is highlighted on some single molecules (marked with solid white circles). Some avidin molecules were not recognized by the biotinylated tip (dashed white circle), which could be caused by a partial loss in the functionality of avidin. The specificity of the recognition signals was proven by a block of the tip with free avidin and repeating of recognition imaging (Figure 8). Figure 8a shows the

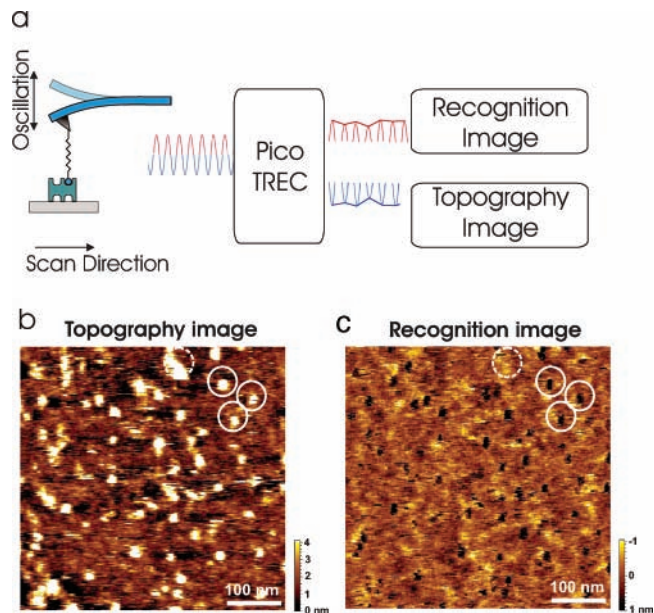


**FIGURE 7.** Simultaneous topography and recognition imaging. (a) Signal processing for simultaneously obtaining topography and recognition images. The raw cantilever deflection signal of the oscillating cantilever is thereby split via the TREC-box into upper parts (corresponding to the recognition image) and lower parts (corresponding to the topography image). (b) Topographical image of avidin molecules adsorbed to mica acquired with a biotin-tethered tip. (c) Simultaneously acquired recognition image. A good correlation between topography and recognition was found (solid circles). Topographical spots without recognition denote structures lacking specific interaction (dashed circle).

recognition image prior to blocking, with a high efficiency of recognition at a high signal-to-noise ratio. Injection of free avidin into the solution resulted in the disappearance of the dark spots in the recognition image (Figure 8b), while the corresponding topography image remained unchanged (not shown). Before blocking, almost all avidin molecules were recognized, while after the block only five

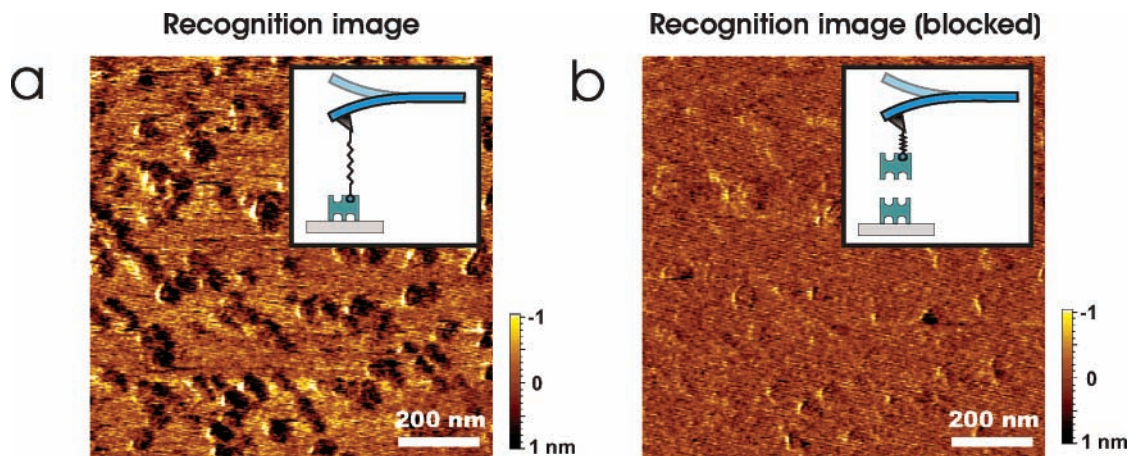


**FIGURE 8.** Demonstrating the specificity of recognition imaging. (a) Recognition image of avidin molecules adsorbed to mica acquired with a biotin-tethered tip, prior to blocking. (b) Recognition image after blocking the tip by adding free avidin into the solution while scanning the same position. Almost all black recognition spots disappeared, proving the specificity of the molecular interaction underlying the recognition image.

spots remained in the recognition image, probably due to adhesive locations on the surface. This specific block demonstrates that the recognition events arise from the interaction of biotin on the tip with avidin on the surface, proving the overall specificity of the detected molecular recognition signals.

In another study, a specific type of molecule (histone H3) in a complex sample of chromatin adsorbed onto a surface was recognized by an anti-histone H3 functionalized tip while simultaneously recording a high-resolution image of the same sample.<sup>34</sup> The recognition spots in the recognition image revealed the locations of histone H3 in the topographical image with high lateral resolution and high efficiency. In addition to the localization of histone H3 in the complex biological sample of chromatin, the compositional changes during histone remodeling were also recorded in the topography and recognition images. The simultaneous investigation of both topography and recognition will open a wide field of applications for investigating biological structure–function relationships in native environments on the nanometer scale, because the technique can map composition on top of a topographical image and can detect compositional changes occurring during biological processes.

## Concluding Remarks

Atomic force microscopy has evolved into an imaging method that yields fine structural details on native biological samples such as proteins, nucleotides, membranes, and cells in their physiological environment and at ambient conditions. Due to its high lateral resolution and sensitive force detection capability, the exciting option of measuring intramolecular forces on the single-molecule level has also become possible. The proof-of-principle stage of the pioneering experiments has already evolved into established methods for exploring kinetic and structural details of interactions and molecular recognition processes. Data obtained from force spectroscopy include physical parameters not measurable by other methods

and opens new perspectives in exploring the regulation of the dynamics of biological processes. New instrumental developments such as the recently developed recognition imaging mode allow the biochemical composition of the sample to be investigated. Together with improvements of the sensitivity and acquisition speed, this has paved the way to exciting fields in nano-bioscience and nano-biotechnology.

*This work was supported by Austrian Science Foundation Projects P14549/P15295, the GEN-AU initiative of the Austrian Ministry of Education, Science and Culture, the Human Frontier Science Program (Grant RG-P0053/2004), and the European Commission (STREP program).*

## References

- (1) Binnig, G.; Quate, C. F.; Gerber, C. Atomic force microscope. *Phys. Rev. Lett.* **1986**, *56*, 930–933.
- (2) Hoerber, J. K.; Miles, M. J. Scanning probe evolution in biology. *Science* **2003**, *302*, 1002–1005.
- (3) Engel, A.; Muller, D. J. Observing single biomolecules at work with the atomic force microscope. *Nat. Struct. Biol.* **2000**, *7*, 715–718.
- (4) Ando, T.; Kodera, N.; Takai, E.; Maruyama, D.; Saito, K.; Toda, A. A high-speed atomic force microscope for studying biological macromolecules. *Proc. Natl. Acad. Sci. U.S.A.* **2001**, *98*, 12468–12472.
- (5) Kienberger, F.; Muller, H.; Pastushenko, V.; Hinterdorfer, P. Following single antibody binding to purple membranes in real time. *EMBO Rep.* **2004**, *5*, 579–583.
- (6) Frederix, P. L.; Akiyama, T.; Staufer, U.; Gerber, C.; Fotiadis, D.; Muller, D. J.; Engel, A. Atomic force bio-analytics. *Curr. Opin. Chem. Biol.* **2003**, *7*, 641–647.
- (7) Florin, E. L.; Moy, V. T.; Gaub, H. E. Adhesion forces between individual ligand receptor pairs. *Science* **1994**, *264*, 415–417.
- (8) Lee, G. U.; Chrisey, A. C.; Colton, J. C. Direct measurement of the forces between complementary strands of DNA. *Science* **1994**, *266*, 771–773.
- (9) Hinterdorfer, P.; Baumgartner, W.; Gruber, H. J.; Schilcher, K.; Schindler, H. Detection and localization of individual antibody–antigen recognition events by atomic force microscopy. *Proc. Natl. Acad. Sci. U.S.A.* **1996**, *93*, 3477–3481.
- (10) Benoit, M.; Gabriel, D.; Gerisch, G.; Gaub, H. E. Discrete interactions in cell adhesion measured by single-molecule force spectroscopy. *Nat. Cell Biol.* **2000**, *2*, 313–317.
- (11) Marzsalek, P. E.; Oberhauser, A. F.; Pang, Y. P.; Fernandez, J. M. Polysaccharide elasticity governed by chair-boat transitions of the glucopyranose ring. *Nature* **1998**, *396*, 661–664.
- (12) Smith, S.; Cui, Y.; Bustamante, C. Overstretching B-DNA: the elastic response of individual double-stranded and single-stranded DNA molecules. *Science* **1996**, *271*, 795–799.

- (13) Veigel, C.; Coluccio, L. M.; Jontes, J. D.; Sparrow, J. C.; Milligan, R. A.; Molloy, J. E. The motor protein myosin-I produces its working stroke in two steps. *Nature* **1999**, *398*, 530–533.
- (14) Evans, E. Probing the relation between force-lifetime and chemistry in single molecular bonds. *Annu. Rev. Biophys. Biomol. Struct.* **2001**, *30*, 105–128.
- (15) Stroh, C. M.; Ebner, A.; Geretschlager, M.; Freudenthaler, G.; Kienberger, F.; Kamruzzahan, A. S. M.; Smith-Gill, S. J.; Gruber, H. J.; Hinterdorfer, P. Simultaneous topography and recognition imaging using force microscopy. *Biophys. J.* **2004**, *87*, 1981–1990.
- (16) Viani, M. B.; Pietrasanta, L. I.; Thompson, J. B.; Chand, A.; Gebeshuber, I. C.; Kindt, J. H.; Richter, M.; Hansma, H. G.; Hansma, P. K. Probing protein–protein interactions in real time. *Nat. Struct. Biol.* **2000**, *7*, 644–647.
- (17) Hinterdorfer, P.; Kienberger, F.; Raab, A.; Gruber, H. J.; Baumgartner, W.; Kada, G.; Riener, C.; Wielert-Badt, S.; Borken, C.; Schindler, H. Poly(ethylene glycol): An ideal spacer for molecular recognition force microscopy/spectroscopy. *Single Mol.* **2000**, *1*, 99–103.
- (18) Hinterdorfer, P.; Schilcher, K.; Baumgartner, W.; Gruber, H. J.; Schindler, H. A mechanistic study of the dissociation of individual antibody–antigen pairs by atomic force microscopy. *Nanobiology* **1998**, *4*, 39–50.
- (19) Riener, C.; Kienberger, F.; Hahn, C. D.; Buchinger, G. M.; Egwim, I. O. C.; Haselgruebler, T.; Ebner, A.; Romanin, C.; Klampfl, C.; Lackner, B.; Prinz, H.; Blaas, D.; Hinterdorfer, P.; Gruber, H. J. Heterobifunctional cross-linkers for tethering single ligand molecules to scanning probes. *Anal. Chim. Acta* **2003**, *497*, 101–114.
- (20) Kienberger, F.; Kada, G.; Gruber, H. J.; Pastushenko, V. P.; Riener, C.; Trieb, M.; Knaus, H. G.; Schindler, H.; Hinterdorfer, P. Recognition force spectroscopy studies of the NTA-His6 bond. *Single Mol.* **2000**, *1*, 59–65.
- (21) Riener, C. K.; Stroh, C. M.; Ebner, A.; Klampfl, C.; Gall, A.; Romanin, C.; Lyubchenko, Y. L.; Hinterdorfer, P.; Gruber, H. J. Simple test system for single molecule recognition force microscopy. *Anal. Chim. Acta* **2003**, *479*, 59–75.
- (22) Grubmüller, H.; Heymann, B.; Tavan, P. Ligand binding: Molecular mechanics calculation of the streptavidin–biotin rupture force. *Science* **1996**, *271*, 997–999.
- (23) Bell, G. I. Models for the specific adhesion of cells to cells. *Science* **1978**, *200*, 618–627.
- (24) Evans, E.; Ritchie, K. Dynamic strength of molecular adhesion bonds. *Biophys. J.* **1997**, *72*, 1541–1555.
- (25) Strunz, T.; Oroszlan, K.; Schumakovitch, I.; Güntherodt, H. G.; Hegner, M. Model energy landscapes and the force-induced dissociation of ligand–receptor bonds. *Biophys. J.* **2000**, *79*, 1206–1212.
- (26) Merkel, R.; Nassoy, P.; Leung, A.; Ritchie, K.; Evans, E. Energy landscapes of receptor–ligand bonds explored by dynamic force spectroscopy. *Nature* **1999**, *397*, 50–53.
- (27) Nevo, R.; Stroh, C.; Kienberger, F.; Kaftan, D.; Brumfeld, V.; Elbaum, M.; Reich, Z.; Hinterdorfer, P. A molecular switch between two bound states in the RanGTP–importin $\beta$ 1 interaction. *Nat. Struct. Biol.* **2003**, *10*, 553–557.
- (28) Willemsen, O. H.; Snel, M. M. E.; van der Werf, K. O.; de Grooth, B. G.; Greve, J.; Hinterdorfer, P.; Gruber, H. J.; Schindler, H.; van Kyook, Y.; Figdor, C. G. Simultaneous height and adhesion imaging of antibody antigen interactions by atomic force microscopy. *Biophys. J.* **1998**, *57*, 2220–2228.
- (29) Radmacher, M.; Cleveland, J. P.; Fritz, M.; Hansma, H. G.; Hansma, P. K. Mapping interaction forces with the atomic force microscope. *Biophys. J.* **1994**, *66*, 2159–2165.
- (30) Ludwig, M.; Dettmann, W.; Gaub, H. E. AFM imaging contrast based on molecular recognition. *Biophys. J.* **1997**, *72*, 445–448.
- (31) Almqvist, N.; Bhatia, R.; Primbs, G.; Desai, N.; Banerjee, S.; Lal, R. Elasticity and Adhesion Force Mapping Reveals Real-Time Clustering of Growth Factor Receptors and Associated Changes in Local Cellular Rheological Properties. *Biophys. J.* **2004**, *86*, 1753–1762.
- (32) Raab, A.; Han, W.; Badt, D.; Smith-Gill, S. J.; Lindsay, S. M.; Schindler, H.; Hinterdorfer, P. Antibody recognition imaging by force microscopy. *Nat. Biotechnol.* **1999**, *17*, 902–905.
- (33) Ebner, A.; Kienberger, F.; Kada, G.; Stroh, C. M.; Geretschlager, M.; Kamruzzahan, A. S. M.; Wildling, L.; Johnson, W. T.; Ashcroft, B.; Nelson, J.; Lindsay, S. M.; Gruber, H. J.; Hinterdorfer, P. Localization of single avidin biotin interactions using simultaneous topography and molecular recognition imaging. *ChemPhysChem* **2005**, *6*, 897–900.
- (34) Stroh, C.; Wang, H.; Bash, R.; Ashcroft, B.; Nelson, J.; Gruber, H. J.; Lohr, D.; Lindsay, S. M.; Hinterdorfer, P. Single-molecule recognition imaging microscope. *Proc. Natl. Acad. Sci. U.S.A.* **2004**, *101*, 12503–12507.

AR050084M